

Map-based UAV mmWave Channel Model and Characteristic Analysis

Shan Jiang¹, Qiuming Zhu^{1,*}, Cheng-Xiang Wang^{2,3,*}, Kai Mao¹, Wenping Xie¹, Weizhi Zhong¹, Mengtian Yao¹

¹The Key Laboratory of Dynamic Cognitive System of Electromagnetic Spectrum Space,
College of Electronic and Information Engineering,

Nanjing University of Aeronautics and Astronautics, Nanjing 211106, China

²National Mobile Communications Research Laboratory, School of Information Science and Engineering,
Southeast University, Nanjing 210096, China

³Purple Mountain Laboratories, Nanjing 211111, China

*Corresponding author

Email: {js0615, zhuqiuming}@nuaa.edu.cn, chxwang@seu.edu.cn,
{maokai, xiewp, zhongwz, yaomengtian}@nuaa.edu.cn

Abstract—In this paper, a new millimeter wave (mmWave) channel model based on the digital map for UAV-to-ground communications is developed. Two key steps to run the proposed model, i.e., the reconstruction of scattering scenario based on the digital map and parameter computation based on the ray-tracing (RT) method, are demonstrated in detail. Based on the proposed channel model, the channel characteristics under different scenarios are analyzed based on the massive RT simulated data. We conduct the RT simulations at the 28 GHz under urban, hilly, forest, and sea scenarios, respectively. The inter-cluster and intra-cluster channel parameters including the cluster number, power gain, delay, and angles are investigated. The simulation and analyze results show that the inter-cluster and intra-cluster channel characteristics are different obviously in different scenarios.

Index Terms—UAV mmWave channel, channel model, ray-tracing (RT), channel characteristic.

I. INTRODUCTION

The fifth generation (5G) systems allow to share information in various scenarios with exceedingly low latency and high transmission rate [1], [2]. In the future 5G systems, the mmWave communication is one of the most prospective techniques. Meanwhile, the unmanned aerial vehicles (UAVs) have been widely applied in communication systems, such as the aerial relay and base station relay, due to their flexibility, portability, and low cost. The mmWave band can be very necessary for UAV communications to satisfy the requirements for 5G high throughput mobile applications and communication quality [3]–[6]. In order to efficiently design and optimize the UAV mmWave communication systems, it is vital to understand and model an accurate and reliable channel model [7]–[10].

The geometry-based stochastic model (GBSM) approach has been widely used in channel modelling and characteristic analysis of UAV communications [11]–[13]. Non-stationary characteristics for UAV channel model were considered in

[14]–[17], but only the channel models in [18], [19] were designed for the mmWave band. So far, only a few works of channel measurements and modeling can be addressed [11], [20], [21]. In [20], the authors provided an experimental setup for air-to-ground (A2G) mmWave channel sounding measurements. In [21], the parameters such as the time delay and power gain of the UAV mmWave channel were studied based on the measured data of the channel at 16 GHz. Although the measurement is a reliable method to know real channel characteristics, it demands a large number of trials and time. The RT simulation is a good choice to reduce this effort.

The authors in [22], [23] showed that the received power results from the RT simulation have a good agreement with measured ones. The authors in [24]–[26] analyzed the mmWave propagation characteristics in urban environment based on RT simulations. Moreover, the propagation characteristics in mountain terrain and suburban environments were also analyzed in [27], [28].

UAV mmWave channels have unique inter-cluster and intra-cluster characteristics, which are caused by high frequency and high time resolution in mmWave bands with large bandwidth. Although channel measurements and characteristic analyzed for UAV channels have been investigated in the literature, the research of these characteristics under different scenarios are still insufficient. This paper aims to make up for this research gap. Firstly, a map-based UAV mmWave model to analyze channel characteristics combined with the RT method is proposed. In order to reduce the complexity of parameter calculation procedure, a scenario reconstruction method is proposed based on the realistic propagation environment. Combined with the RT method, aimed at four scenarios of urban, hilly, forest, and sea, inter-cluster and intra-cluster channel parameters, i.e., cluster number, power, delay, and angles are analyzed and compared based on massive RT simulations.

The remained paper is organized as follows. The map-based channel model is developed in Section II. The detailed reconstruction process of scenarios and the RT technology are demonstrated in Section II. Four different communication scenarios of urban, hilly, forest, and sea are constructed and massive simulations are conducted in Section III. The analysis results of inter-cluster and intra-cluster are also shown in Section III. Some conclusions are given in Section IV.

II. MAP-BASED UAV MMWAVE CHANNEL MODELING

A. Flowchart of channel modeling

Under the 3D propagation environment, the channel impulse response (CIR) of UAV mmWave channels should consider the impacts of propagation on both azimuth and elevation planes and can be expressed as

$$h(t, \Theta, \Phi) = \sum_{n=1}^N \sum_{k=1}^{M_n} a_{nk} \cdot \delta(t - \tau_{nk}(t)) \cdot \delta(\Theta - \Theta_{nk}(t)) \cdot \delta(\Phi - \Phi_{nk}(t)) \quad (1)$$

where the subscript $(\cdot)_{nk}$ represents the k th ray within the n th cluster. In addition, a and τ are the power gain and delay of a ray. Vectors Θ_{nk} , Φ_{nk} are AoD and AoA directions, respectively. The AoD direction $\Theta_{nk}(t) = (\alpha_{nk}^{\text{tx}}(t), \beta_{nk}^{\text{tx}}(t))$ is a vector containing azimuth and elevation angle of arrival. Similarly, the AoA $\Phi_{nk}(t) = (\alpha_{nk}^{\text{rx}}(t), \beta_{nk}^{\text{rx}}(t))$ is a vector containing azimuth and elevation angle of departure. It should be noticed that different numbers of rays are assumed in different clusters. Therefore, the number of rays M_n within the n th cluster is depending on n . The number of clusters is expressed as N . It should be noticed that the numbers of ray for each cluster are different.

Our next task is to determine the channel parameters, i.e., power gain, time delay, AoDs, and AoAs for the above model. The propagation rays include the direct, reflected, diffracted, scattered, and some combined rays. RT method is based on the geometrical optics, uniform theory of diffraction (UTD), and field intensity superposition principle. It is useful and accurate to analyze the channel parameters in high frequency band such as mmWave. It was also found that calculating the channel parameters by the RT method under a realistic 3D propagation environment often needs huge computation resources due to the geometric and physical complexity of scattering environments [29], [30]. To overcome this shortcoming, a simplify algorithm is adopted in this paper, which only considers the main rays or the main geometric and physical characteristics of scatterers.

The main flowchart to run our proposed channel model includes two steps, i.e., reconstruction of scatterers including terrain, buildings and trees, and parameter computation. The reconstruction step is very important and also flexible to balance the complexity and accuracy. Note that the computation method covers the geometric parameters and channel parameters according to the locations of transceivers and scattering environments.

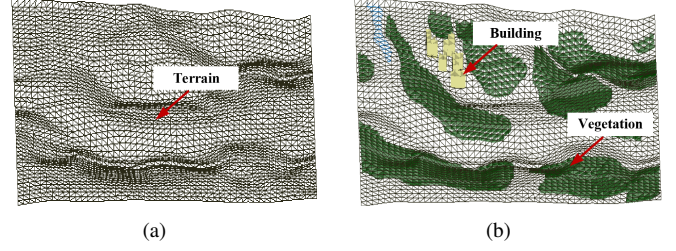


Fig. 1. Reconstructed terrain, buildings and vegetation

B. Scattering scenario reconstruction

In order to reduce the complexity, the realistic propagation environment must be properly reconstructed based on the original map. In this paper, we reconstruct the database of buildings and terrain by following steps.

Firstly, we get the original digital terrain model (DEM) of interesting area which includes the details about latitude, longitude, and elevation of all points. The ray traverses the whole surface to find the point of intersection of the ray and the grid.

Then, we approximate all walls with complex structures by simple structure based on the 2D database of buildings. Based on this, the measured height information can be used to obtain 3D building database and superimposed on the terrain.

Finally, in order to simplify the tracing procedure of all rays, we use many triangle facets to describe the surface of terrain, building, and etc. The triangulation of terrain with buildings and vegetation is shown in Fig.1.

C. RT-based parameter calculation

Based on the reconstructed digital map, each ray is tracked from the source by RT techniques and only the rays that contribute to the electric field strength on the receiving point are chosen. Since the electromagnetic propagation process can be divided into three cases, i.e., direction, reflection, and diffraction, different methods are needed to calculate the relevant electric field intensity.

For the direct ray, it can be directly connected according to the coordinate information of the transmitter and receiver. The electric field intensity can be calculated by

$$E_0(t) = E^{1m} \frac{e^{-jk d_0^{\text{tx}}(t)}}{d_0^{\text{tx}}(t)} \quad (2)$$

where E^{1m} is the electric field intensity of 1 m from the transmitter, k is the wave number and $d_0^{\text{tx}}(t)$ is the distance between the UAV and Rx.

For the reflection ray, the calculation formula of electric field intensity can be described as

$$E_l^{\text{R}}(t) = E_0 R \frac{e^{-lk(d_l^{\text{tx},S}(t) + d_l^{\text{S},\text{rx}}(t))}}{d_l^{\text{tx},S}(t) + d_l^{\text{S},\text{rx}}(t)} \quad (3)$$

where R is reflection coefficient, $d_l^{\text{tx},S}(t)$ is the distance between the UAV and scatterer, $d_l^{\text{S},\text{rx}}(t)$ is the distance between the Rx and scatterer.

According to the UTD theory, the electric field intensity of diffracted ray can be expressed as

$$E_l^D(t) = \frac{E_0}{d_l^{S,rx}(t)} D \sqrt{\frac{d_l^{S,rx}(t)}{d_l^{t,x,S}(t) \cdot (d_l^{t,x,S}(t) + d_l^{S,rx}(t))}} \cdot e^{-jk(d_l^{t,x,S}(t) + d_l^{S,rx}(t))} \quad (4)$$

where D is diffraction coefficient.

III. CHANNEL CHARACTERISTIC ANALYZE BASED ON RT SIMULATIONS

A. RT simulation setup

We consider four typical communication scenarios for ray tracing simulations, i.e., urban, hilly, forest, and sea as shown in Fig.2. The key factors for A2G communication scenarios are the scatterers around the receiver and the terrain. For the urban scenario, the buildings with different height and structure are densely distributed, and the average height of buildings is about 50 m. For the hilly scenario, the terrain is undulating. For the forest scenario, the terrain is approximately flat and covered with vegetation with the height of 15m. For the sea scenario, there are few buildings. We considered the material of all the buildings as concrete for simplify. Moreover, for all the land-based simulations, wet soil is considered.

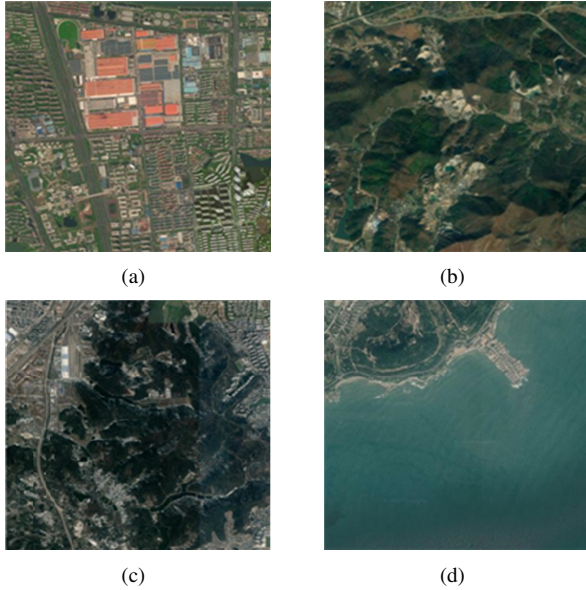


Fig. 2. Satellite view of (a) urban, (b) hilly, (c) forest, and (d) sea.

In order to obtain the statistical properties, we set up 9 ground positions as receivers and 200 aerial positions as transmitters as shown in Fig. 3. In the RT simulations, each ray can experience 6 reflections, 2 diffractions, and 1 diffuse reflection at most, which is an adequate tradeoff between computation efficiency and results accuracy. The rest simulation parameters are described in Table 2.

B. RT data fitting and analyze

Channel parameters such as the power, delay, phase, and angle of each ray can be obtained via the RT method. Each

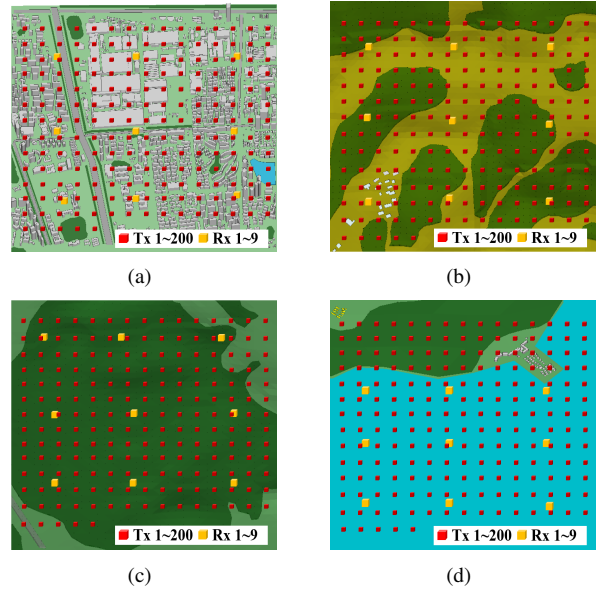


Fig. 3. Reconstruction scenarios of (a) urban, (b) hilly, (c) forest and (d) sea

TABLE I
SIMULATION PARAMETERS.

Parameter	Value
Frequency	28 GHz
Bandwidth	500 MHz
Transmitting power	20 dBm
Antenna type	omnidirectional
UAV height	150 m
Vehicle height	2 m
UAV speed	10 m/s

ray gets reflected, diffracted or scattered due to all kinds of obstacles along their path to the receiver. Therefore, the rays reaching the receiver are characterized by different delays, powers, and angles. In the simulation, the rays with the power below -25 dB compared with the first non-light-of-sight (NLoS) ray are ignored.

After obtaining data of each ray, a clustering algorithm is needed to group these rays into several clusters. The clustering of rays relies on their delays, powers, and angles. Here, the nearest neighbor algorithm is employed to analyze the valid cluster number. In this paper, Euclidean distance is used as the metric for clustering. Let $T = 15$ be the threshold of clustering. The first ray is taken as the first centroid. Then, it groups a ray into a cluster by compare the Euclidean distance and threshold. Next, it groups a ray into a cluster by comparing the Euclidean distance and threshold. The Euclidean distance of j th ray and k th centroid can be described as

$$ED_j = \sqrt{S(\tau_j - \tau_k)^2 + (\alpha_j - \alpha_k)^2 + (\beta_j - \beta_k)^2} \quad (5)$$

where S is a scaling coefficient, τ_k , α_k and β_k are the delay, azimuth angle of arrival (AAOA), and elevation angle of arrival (EAOA) of the k th centroid, τ_j , α_j and β_j are the

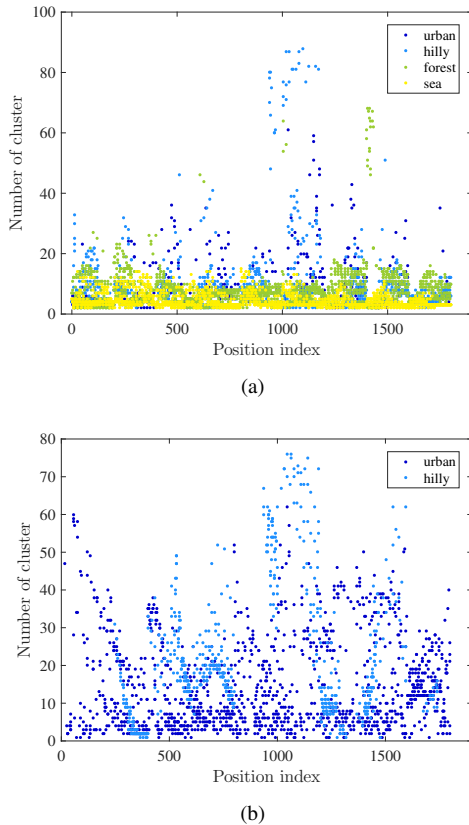


Fig. 4. Average numbers of valid cluster for (a) LoS and (b) NLoS cases.

delay, AOA, and elevation EAOA of the j th ray. If the Euclidean distance is greater than the threshold, a new centroid is generated. Finally, the cluster number K can be determined.

Clustering is important for analyzing the characteristics of cluster. The determination on the number of clusters strongly depends on the cluster definition and environments. In order to obtain the statistical properties of cluster for different scenarios, we choose 9 ground receivers and 200 aerial transmitters, i.e., totally 1800 A2G channels. The average number of valid clusters under different scenarios are obtained and compared in Fig. 4. For LoS cases, it can be found that the number in urban, hilly, and forest scenarios is mainly 0~15, while it is 0~10 in the sea scenario. For NLoS cases, the number is concentrated in 0~20 in urban scenario, and 0~30 in the hilly scenario. The distributions of cluster number under different scenarios are compared in Fig. 5. The cluster number of each scenario is obtained by averaging 1800 channels. Moreover, the mean values of LoS case are 9.7, 9.9, 8.0, and 4.3, while they are up to 14.5 and 21.1 for the NLoS urban and hilly scenarios.

The delay and power of each cluster are important for evaluating the quality of fading channels. The time delay in Fig. 6 (a) shows that it ranges from 0 ns to 3000 ns and mainly concentrates between 0 ns and 1000 ns. As we can see that it obeys the exponential distribution which is similar with the recommendations in [31]. The attenuation coefficients of fitted

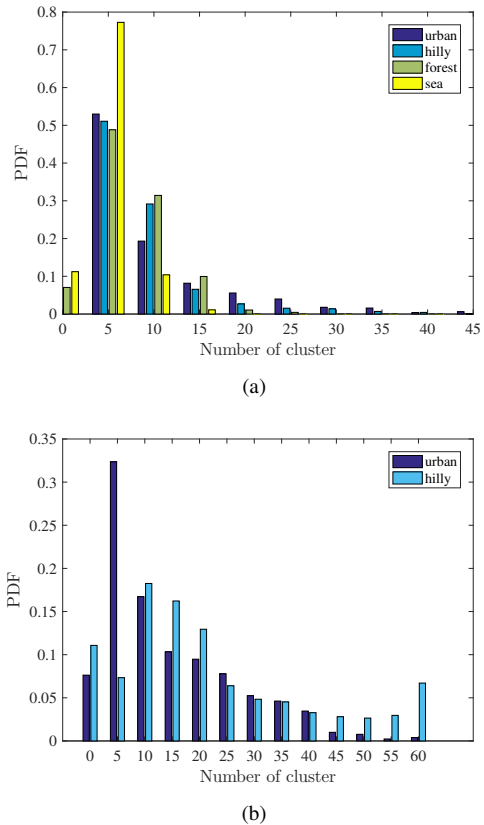


Fig. 5. Distributions of cluster number under the (a) LoS and (b) NLoS cases.

curves are 0.39, 1.78, 1.52, and 1.67, respectively. The PDPs that based on a large amount of simulation data are given in Fig. 6 (b).

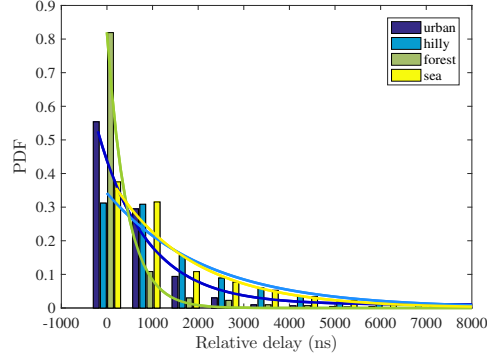
The relative delay means the offset values of each intra-cluster ray delay on the mean cluster delay. The definition of relative azimuth and elevation are similar. Under the LoS case, the PDF of relative delay and AoA are given in Fig.7 (a) and Fig.7 (b), respectively. We found that the PDFs of relative delay, relative azimuth, and relative elevation can be fitted well by the lognormal distribution. The probability density function can be expressed as

$$f(x) = \frac{1}{\sqrt{2\pi}\sigma} \exp\left(-\frac{(\ln x - \mu)^2}{2\sigma^2}\right) \quad (6)$$

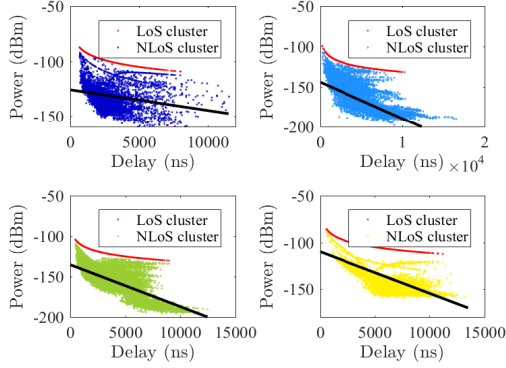
where x follows a lognormal distribution, with mean of μ , and variance of σ^2 . The mean and standard deviation of the fitted curves in different scenarios are shown in Table 2. Note that the distribution of relative azimuth and elevation in urban is significantly different with others due its rich scatterers.

IV. CONCLUSIONS

In this paper, we have developed a UAV mmWave channel model and analyzed its channel characteristics based on massive RT simulations. Since complex databases may take hours for the RT simulation, a scenario reconstruction method is demonstrated. Based on the four reconstructed scenarios of



(a)



(b)

Fig. 6. (a) The PDF and (b) the PDP of delay under the LoS case.

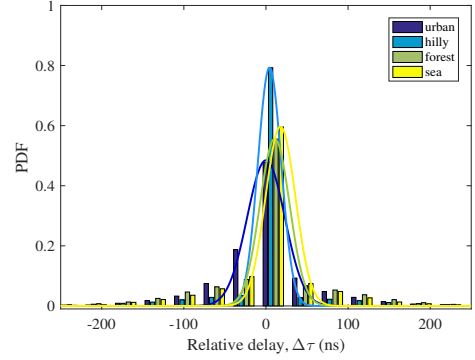
TABLE II
PARAMETERS IN THE SIMULATION FOR DELAY AND ANGLE

Scenarios		Urban	Hilly	Forest	Sea
Relative delay	μ_τ	1.21	1.98	1.39	1.41
	σ_τ	22.6	14.1	18.9	18.26
Relative azimuth	μ_α	0.76	1.87	1.87	1.625
	σ_α	1.85	0.59	1.05	0.997
Relative elevation	μ_β	1.94	2.2	1.89	2.17
	σ_β	3.56	0.79	0.926	0.85

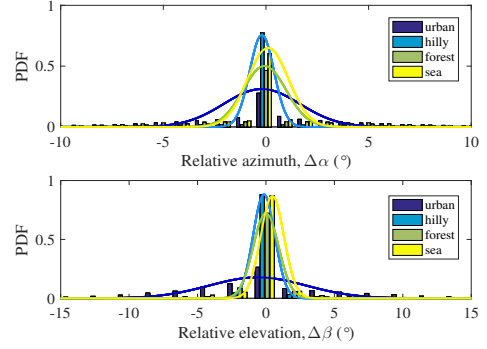
urban, forest, hilly, and sea, channel characteristics parameters of inter-cluster and intra-cluster at 28 GHz for UAV channel have been analyzed. The results analysis is based on data obtained by RT simulations. The simulation results have shown that the channel characteristics of different scenarios are different obviously due to the effects of scatterers. The model and simulation method can be used to evaluate the channel characteristics of UAV mmWave communication systems, and provide theoretical basis for optimizing the UAV system design.

ACKNOWLEDGMENT

This work was supported by the National Key R&D Program of China (No. 2018YF1801101), the National Natural Science Foundation of China (No. 61960206006), the EU



(a)



(b)

Fig. 7. PDFs of relative (a) delay and (b) azimuth and elevation under the LoS case.

H2020 RISE TESTBED2 project (No. 872172), the Aeronautical Science Foundation of China (No. 201901052001), the Fundamental Research Funds for the Central Universities (No. NS2020026 and No. NS2020063) and the National Key Scientific Instrument and Equipment Development Project (No. 61827801).

REFERENCES

- [1] Y. Liu, C.-X. Wang, C. F. Lopez, G. Goussetis, Y. Yang, et al., "3D non-stationary wideband tunnel channel models for 5G high-speed train wireless communications," *IEEE Trans. Intell. Transp. Syst.*, vol. 21, no. 1, pp. 259–272, Jan. 2020.
- [2] C.-X. Wang, J. Bian, J. Sun, W. Zhang, and M. Zhang, "A survey of 5G channel measurements and models," *IEEE Commun. Surv. Tuts.*, vol. 20, no. 4, pp. 3142–3168, Aug. 2018.
- [3] L. Bin, F. Zesong, and Z. Yan, "UAV communications for 5G and beyond: recent advances and future trends," *IEEE Internet Things J.*, vol. 6, no. 2, pp. 2241–2263, Dec. 2018.
- [4] W. Fan, I. Carton, P. Kyosti, A. Karstensen, T. Jamsa, et al., "A step toward 5G in 2020: low-cost OTA performance evaluation of massive MIMO base stations," *IEEE Antennas Propag. Mag.*, vol. 59, no. 1, pp. 38–47, Feb. 2017.
- [5] J. Zhang, M. Shafi, A. Molisch, F. Tufvesson, S. Wu, et al., "Channel models and measurements for 5G," *IEEE Commun. Mag.*, vol. 56, no. 12, pp. 12–13, Dec. 2018.
- [6] L. Bai, C.-X. Wang, G. Goussetis, S. Wu, Q. Zhu, et al., "Channel modeling for satellite communication channels at Q-band in high latitude," *IEEE Access*, vol. 7, no. 1, pp. 137691–137703, Dec. 2019.
- [7] Z. Ullah, F. Al-Turjman and L. Mostarda, "Cognition in UAV-Aided 5G and Beyond Communications: A Survey," *IEEE Transactions on Cognitive Communications and Networking*, to be published.

- [8] Q. Zhu, Y. Wang, K. Jiang, X. Chen, W. Zhong, et al., "3D non-stationary geometry-based multi-input multi-output channel model for UAV-ground communication systems," *IET Microw., & Antennas Propag.*, vol. 8, no. 13, pp. 1104–1112, Apr. 2019.
- [9] W. Zhong, L. Xu, Q. Zhu, X. Chen, and J. Zhou, "MmWave beamforming for UAV communications with unstable beam pointing," *China Commun.*, vol. 16, no. 1, pp. 37–46, Jan. 2019.
- [10] X. Chen, X. Hu, Q. Zhu, W. Zhong, B. Chen, "Channel Modeling and Performance Analysis for UAV Relay Systems," *China Commun.*, vol. 15, no. 12, pp. 89–97, Sep. 2018.
- [11] R. Jia, Y. Li, X. Cheng, and B. Ai, "3D geometry-based UAV-MIMO channel modeling and simulation," *China Commun.*, vol. 15, no. 12, pp. 64–74, Dec. 2018.
- [12] K. Jin, X. Cheng, X. Ge, X. Yin, "Three dimensional modeling and space-time correlation for UAV channels," in *Proc. VTC Spring'17*, Sydney, NSW, Australia, June 2017, pp. 1–5.
- [13] H. Jiang, Z. Zhang, L. Wu and J. Dang, "Three-Dimensional Geometry-Based UAV-MIMO Channel Modeling for A2G Communication Environments," *IEEE Commun. Lett.*, vol. 22, no. 7, pp. 1438–1441, July 2018.
- [14] H. Chang, J. Bian, C.-X. Wang, Z. Bai, W. Zhou, et al., "A 3D non-stationary wideband GBSM for low-altitude UAV-to-ground V2V MIMO channels," *IEEE Access*, vol. 7, pp. 70719–70732, May 2019.
- [15] Q. Zhu, K. Jiang, X. Chen, W. Zhong, and Y. Yang, "A novel 3D non-stationary UAV-MIMO channel model and its statistical properties," *China Commun.*, vol. 15, no. 12, pp. 147C-158, Dec. 2018.
- [16] Q. Zhu, Y. Yang, C. -X. Wang, Y. Tan, J. Sun, et al. "Spatial correlations of a 3-D non-stationary MIMO channel model with 3-D antenna arrays and 3-D arbitrary trajectories," *IEEE Wirel. Commun. Le.*, vol. 8, no. 2, pp. 512–515, Apr. 2019.
- [17] X. Cheng, and Y. Li, "A 3-D Geometry-Based Stochastic Model for UAV-MIMO Wideband Nonstationary Channels," *IEEE Internet Things J.*, vol. 6, no. 2, pp. 1654–1662, Apr. 2019.
- [18] J. Zhao, F. Gao, L. Kuang, Q. Wu and W. Jia, "Channel Tracking With Flight Control System for UAV mmWave MIMO Communications," *IEEE Commun. Lett.*, vol. 22, no. 6, pp. 1224–1227, June 2018.
- [19] E. T. Michailidis, N. Nomikos, P. Trakadas, and A. G. Kanatas, "Three-Dimensional Modeling of mmWave Doubly Massive MIMO Aerial Fading Channels," *IEEE T. Veh. Technol.*, vol. 69, no. 2 pp. 1190–1202, Feb. 2020.
- [20] W. Khawaja, O. Ozdemir, and I. Guvenc, "UAV air-to-ground channel characterization for mmWave systems," in *Proc. VTC-Fall'17*, Toronto, Canada. Feb. 2017, pp. 1–5.
- [21] R. Geise, A. Weiss, and B. Neubauer, "Modulating Features of Field Measurements with a UAV at Millimeter Wave Frequencies," in *Proc. CAMA'18*, Vasteras, Sweden, Sept. 2018, pp. 1–4.
- [22] M. Jung, J. H. Kim, J. S. Kim, W. H. Jeong, and K. Kim, "The Path Loss Characteristics for New Wireless Mobile Communication System in Outdoor Environments," *Proc. EuMC'12*, Amsterdam, Netherlands, Nov. 2012, pp. 1–6.
- [23] Z. Wang, E. K. Tameh, and A. R. Nix, "Statistical Peer-to-Peer Channel Models for Outdoor Urban Environments at 2 GHz and 5GHz," in *Proc. IEEE VTC-Fall'04*, Los Angeles, CA, USA, Sep. 2004, vol. 7, pp. 5101–5105.
- [24] L. Cheng, Q. Zhu, C. Wang, W. Zhong, B. Hua, et al., "Modeling and Simulation for UAV Air-to-Ground mmWave Channels," in *Proc. EuCAP'20*, Copenhagen, Denmark, Mar. 2020, pp. 1–5.
- [25] P. Alberto, A. Fouda, and A. S. Ibrahim. "Ray tracing analysis for UAV-assisted integrated access and backhaul millimeter wave networks," in *Proc. WoWMoM'19*, Washington, DC, USA, Aug. 2019, pp. 1–5.
- [26] G. Yang, Y. Zhang, Z. He, J. Wen, Z. Ji, et al., "Machine-learning-based prediction methods for path loss and delay spread in air-to-ground millimeter-wave channels," *IET Microw., & Antennas Propag.*, vol. 13, no. 8, pp. 1113–1121, June 2019.
- [27] Z. Cui, K. Guan, D. He, B. Ai, and Z. Zhong, "Propagation Modeling for UAV Air-to-Ground Channel Over the Simple Mountain Terrain," in *Proc. ICC Workshops'19*, Shanghai, China, July 2019, pp. 1–6.
- [28] X. Chu, C. Briso, D. He, X. Yin, and J. Dou, "Channel modeling for low-altitude UAV in suburban environments based on ray tracer," in *Proc. EuCAP'18*, London, UK, Apr. 2018, pp. 1–4.
- [29] Z. Liu, D. Shi, Y. Gao, C. Yuan, J. Bi, et al., "A new ray tracing acceleration technique in the simulation system of electromagnetic situation," in *Proc. CEEM'15*, Hangzhou, China, Nov. 2015, pp. 329–333.
- [30] Q. Zhu, S. Jiang, C.-X. Wang, B. Hua, K. Mao, et al., "Effects of Digital Map on the RT-based Channel Model for UAV mmWave Communications," in *Proc. IWCMC'20*, Limassol, Cyprus, June 2020, pp. 1–6.
- [31] 3GPP, "Study on channel model for frequencies from 0.5 to 100 GHz(Release 16)," 3rd Generation Partnership Project (3GPP), Tech. Rep. [Online]. Available: <http://www.3gpp.org/>. Accessed: Dec., 2019.